Hindawi
Geofluids
Volume 2019, Article ID 4176535, 11 pages
https://doi.org/10.1155/2019/4176535

Research Article

Time Characteristics of the Influence Radius by Injecting N_2 to Displace Coalbed Methane: A Case Study

Chen Li-wei,[1,2] **Yang Tian-hong**,[1] **Yang Hong-min**,[2] **and Wang Li-guo**[2]

[1]*College of Resources and Civil Engineering, Northeastern University, Shenyang 110819, China*
[2]*School of Safety Science and Engineering, Henan Polytechnic University, Jiaozuo, Henan 454000, China*

Correspondence should be addressed to Yang Tian-hong; jjmksgt@126.com

Received 5 July 2018; Revised 8 October 2018; Accepted 18 October 2018; Published 7 February 2019

Guest Editor: Fangtian Wang

Injecting N_2 to displace methane is an effective way to enhance coalbed methane drainage, and the influence radius of this process is an important factor in borehole arrangement. To determine reasonable spacing between injection boreholes and discharge boreholes, experimental and theoretical studies were carried out. The change of rule for the influence radius was determined based on the flow rate changes at the discharge boreholes when injecting gas into a coal seam in the field. Based on gas seepage-diffusion theory, a model for injecting N_2 to displace coalbed methane was established. Through numerical simulation, the time characteristics of the influence radius were analyzed. The results show the following: Under different gas injection pressure conditions, the influence radius increases exponentially as injection time increases, but the rate of increase of the influence radius decreases gradually. For the same injection time, the higher the injection pressure, the wider the influence radius will be. After obtaining field results, regression analysis was applied to analyze the numerical results of gas injection at different pressures, and then, the quantitative relationship between the injection influence radius r, the injection time t, and the injection pressure p was found. According to the results calculated using this formula at an injection pressure of 0.5 MPa, the optimum spacing between boreholes was determined to be 1.5 m at the Shigang Coal Mine. The analysis of reasonable spacing between injection and extraction boreholes at different injection pressures shows that the reasonable spacing between boreholes was linearly correlated with gas injection pressures. This study has important theoretical and practical significance for the spacing between boreholes in a reasonable arrangement when injecting N_2 to displace methane.

1. Introduction

As the main greenhouse gas, efforts to reduce CO_2 emissions from the combustion of fossil fuels have received increasing attention due to concerns over global climate change in recent years [1–3]. In particular, the injection of CO_2 into the deep coal seams to enhance coalbed methane (ECBM) has been an efficient method for the CO_2 capture, utilization, and sequestration (CCUS) engineering [4–8]. In addition, another alternative method to enhance the CBM recovery is to inject the N_2 into coal seams, which can efficiently reduce the partial pressure of CH_4 in the adsorption equilibrium conditions and ultimately enhance the CH_4 desorption from the surfaces of the micro- and mesopores in coal.

At the end of the 20th century, CO_2 was injected for increasing coalbed methane (CO_2-ECBM) in the United States San Juan Basin; this approach was the prelude to CBM coalbed gas injection in the field driving the technology for methane [9–11]. In subsequently years, the United States [9, 12, 13], Canada [14], Japan [5], EU [15], and China [16–18] have started research and have conducted ECBM field trials of various sizes. The US carried out CO_2-ECBM field test in San Juan Basin, Black Warrior Basin, Illinois Basin, and Central Appalachian Basin. In Hokkaido, Japan, Poland, and Alberta, Canada, field trials of different sizes were also carried out. China United Coalbed Methane Co. Ltd. was the first mine that conducted CO_2 injection into the ground in Jincheng, China. Next, China carried out the low-pressure (<0.6 MPa) N_2-ECBM test in Pingdingshan Coal Mine and Yangquan Coal Mine.

With the development of coalbed gas injection technologies to promote gas drainage, scholars conducted many

experimental and theoretical studies, and their studies played an active part in the popularization and application of the technology [19–25]. However, when the technology for gas injection to drain methane was used in coal mines, there were few reports on the reasonable arrangement of injection boreholes and the spacing of discharge boreholes. These arrangements influence the gas displacement effect. If the borehole spacing is too large, it is easy to form blind areas in the elimination outburst area, and if the spacing is too small, it is likely to waste manpower and material resources. The arrangement of injection borehole spacing depends on the influence radius of the borehole. The time characteristic is another important part of reasonable gas injection methods. Thus, the influence radius of injection borehole and its time characteristic need to be addressed.

2. The Basic Theory of Coalbed Methane Flow

2.1. The Gas Diffusion Equation. Assuming that the movement of adsorption gas desorbing from the coal micropore and moving to the fissure system follows Fick diffusion law, then the equation for CH_4 and N_2 diffusing in the pore system is

$$\left(\frac{\partial c_i}{\partial t} + \nabla\right)(-D_i \nabla c_i) = -Q_i \quad (i = 1, 2). \tag{1}$$

In the equation, i represents the gas composition, where $i = 1$ represents CH_4 and $i = 2$ represents N_2. c_i is the concentration of gas in kg/m^3. D_i represents the diffusion coefficient of the gas composition in m^2/s. Q_i is the converged item in kg/(m^3·s), reflecting the mass exchange of the matrix between the adsorption state in the pore system and the free state in the fissure system.

2.2. Gas Seepage Equation [11]. Assuming that the migration of free gas in the coal seam can be treated as a fluid filtration process, then the mass conservation equation [26] of gas seepage in the coal is

$$\left(\frac{\partial m_i}{\partial t} + \nabla\right)(\rho_i v) = Q_i \quad (i = 1, 2). \tag{2}$$

In the equation, ρ_i is the density of the gas composition in kg/m^3 and v is the overall gas seepage speed in m/s; because the seepage of gas in the coal seam follows Darcy's law, the overall flow velocity v can be expressed as

$$v = -\frac{k}{\mu_i}\nabla p. \tag{3}$$

In the equation, k is the permeability of coal in m^2, μ_i is the dynamic viscosity of gas component in N·s/m^2, and ∇p is the pressure gradient in Pa/m.

m_i is the content of the gas composition i in kg/m^3; $m_i = \phi\rho_i$, where ϕ is porosity.

2.3. Adsorption Balance Equations of Multiple Gases. The components of the adsorption state under the hypothetical equilibrium pressure p_i can be represented by the generalized Langmuir equation as follows:

$$c_{p_i} = \rho_{ia}\rho_c \frac{a_i b_i p_i}{1 + b_1 p_1 + b_2 p_2}. \tag{4}$$

In this formula, ρ_{ia} is the density of the gas composition under standard conditions in kg/m^3, ρ_c is the density of the coal in kg/m^3, a_i is the limiting amount of adsorbed gas when the component is adsorbed alone in the coal seam in m^3/kg, and b_i is the component adsorption equilibrium constant in MPa^{-1}. Finally, p_1 and p_2 are the equilibrium pressures of components 1 and 2, respectively, in MPa.

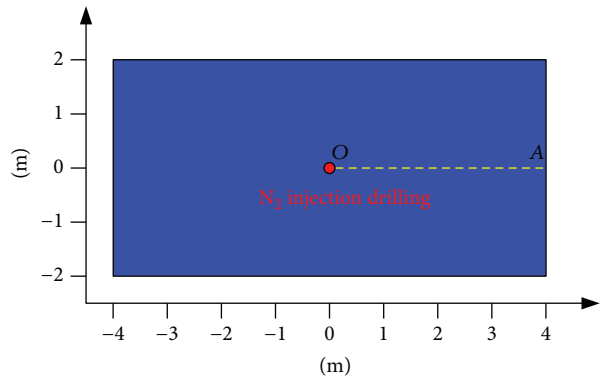

Figure 1: Model for the numerical simulation.

2.4. Mass Exchange Equation. The mass exchange between an adsorption state on the coal surface and a free state in the fissure system can be defined as

$$Q_i = (c_i - c_{pi})\tau. \tag{5}$$

In the equation, τ is desorption diffusion coefficient and represents the difficulty of the adsorption state gas desorbing and diffusing in the fracture system.

2.5. The Gas State Equation. Because the injection pressure is usually not large, the compressibility of the gas is ignored. Considering the gas component as an ideal gas, the ideal gas state equation can be represented as

$$\rho_{ia} = \frac{M_i p_a}{R_i T_a}. \tag{6}$$

In the equation, M_i is the molecular weight of the gas component i, P_a is the gas pressure under the standard condition of 0.1 MPa, and T_a is the gas temperature under the standard condition of 273 K.

2.6. Coupling Equation. Plugging equations (4)~(6) into equation (2), the result is

$$\frac{\phi M_i}{R_i T}\frac{\partial p_i}{\partial t} - \nabla\left(\frac{M_i k p_i}{R_i T \mu_i}\nabla p\right) = Q_i. \tag{7}$$

Table 1: Parameters of physical properties in numerical simulation.

Symbol	Parameter	Number	Unit	Symbol	Parameter	Number	Unit
ρ_c	Coal density	1.35×10^3	kg/m^3	φ	Coal porosity	0.05	
ρ_{1a}	CH_4 density	0.717	kg/m^3	ρ_{2a}	N_2 density	1.25	kg/m^3
μ_1	CH_4 dynamic viscosity coefficient	1.04×10^{-5}	Pa·s	μ_2	N_2 dynamic viscosity coefficient	1.69×10^{-5}	Pa·s
a_1	CH_4 Langmuir constant	0.03832	m^3/kg	a_2	N_2 Langmuir constant	0.01658	m^3/kg
b_1	CH_4 Langmuir constant	0.51	1/MPa	b_2	N_2 Langmuir constant	0.46	1/Mpa
k	Permeability of coal	2.6×10^{-16}	m^2	p_a	Gas pressure under standard conditions	0.1	MPa

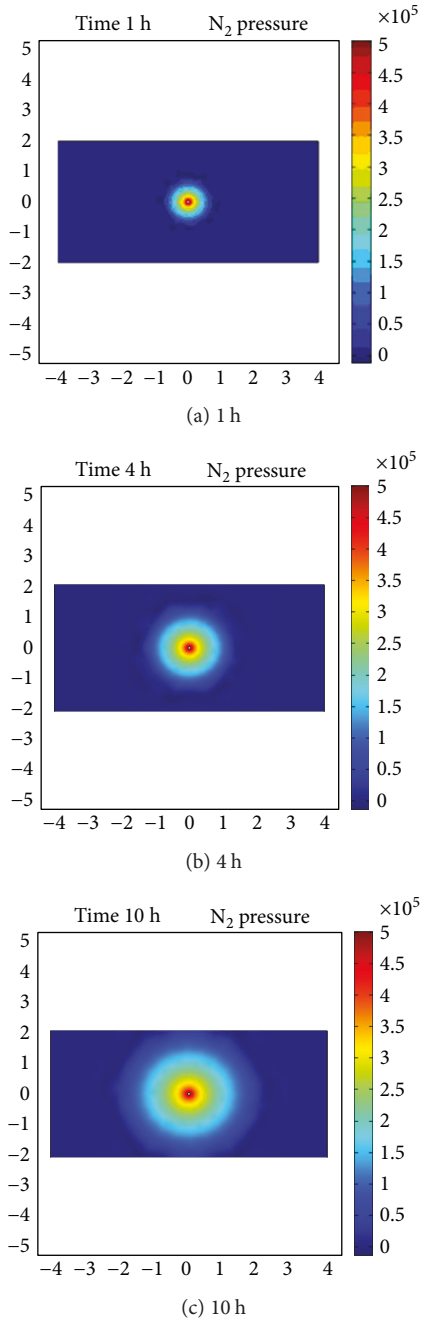

Figure 2: N_2 pressure in coalbed around the borehole at different times under 0.5 MPa gas injection pressure.

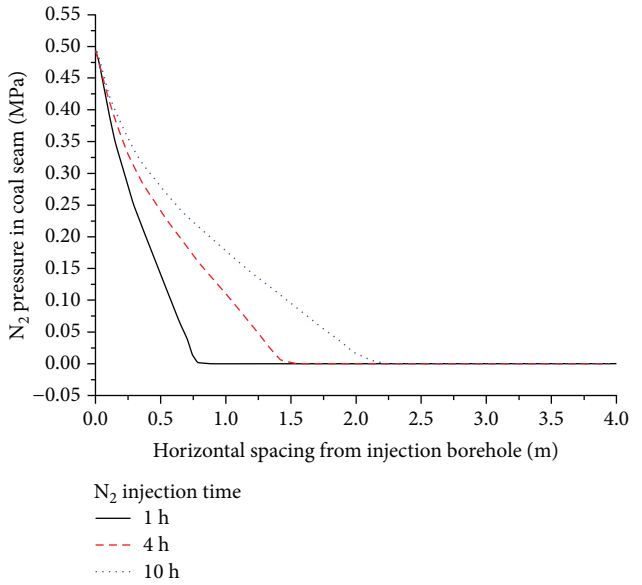

Figure 3: N_2 pressure along the *O-A* direction under 0.5 MPa gas injection pressure.

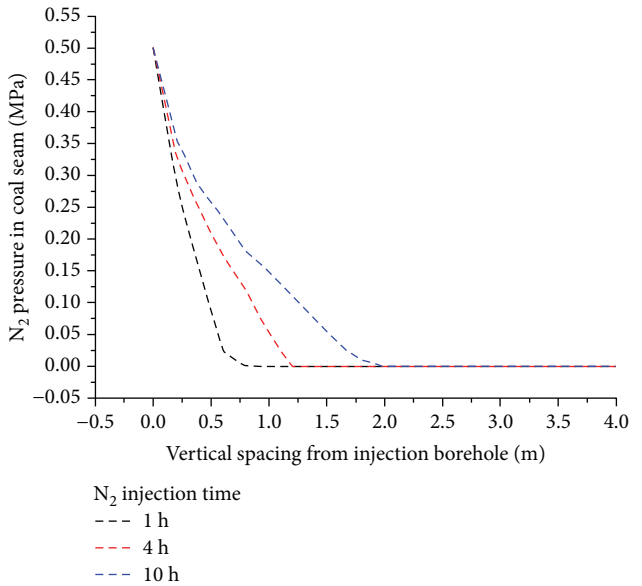

Figure 4: N_2 pressure perpendicular to the *O-A* direction under 0.5 MPa gas injection pressure.

Table 2: The comparison table of gas injection influence radius in vertical and horizontal directions.

Classification	Injection time (h)									
	1	2	3	4	5	6	7	8	9	10
Radius in horizontal direction (m)	0.75	1.00	1.20	1.40	1.50	1.70	1.80	1.90	1.90	2.10
Radius in vertical direction (m)	0.63	0.84	1.05	1.23	1.34	1.49	1.60	1.68	1.70	1.85
Difference (m)	0.12	0.16	0.15	0.17	0.16	0.21	0.20	0.22	0.20	0.25

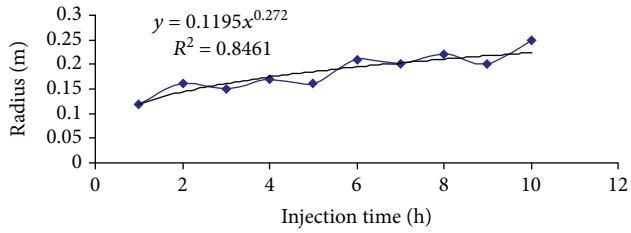

Figure 5: Difference between the horizontal and vertical distances with injection time.

Equations (1) and (7) constitute the continuity equations of multicomponent gas diffusion and seepage in a pore fissure system.

3. Numerical Simulation of Influence Radius by Injecting N_2 to Displace Coalbed Methane

3.1. Experiment Mine. In this paper, Shigang Coal Mine is selected to carry out the test. The Shigang Coal Mine is located in the northeast of the Qinshui Basin in China; the geological structure of the coal seam is complex. The thickness of the no. 15 coal seam, respectively, is 5.93-8.22 m, and its dip angle is approximately 8°. The gas content of the no. 15 coal seam is 10.71-15.21 m^3/t, and the maximum methane pressure is 0.76 MPa.

3.2. Mathematical Model

3.2.1. Basic Assumptions. To build a numerical model for injecting N_2 displacement of coalbed methane, the following basic information needs to be assumed: (1) The in situ stress condition and the anisotropy of the coal seam is neglected. (2) The original gas pressure and gas content in coal seam are the same everywhere. (3) Gas flow in the coal seam is an isothermal process. Adsorption and desorption conform to the generalized Langmuir isothermal adsorption equation. (4) In the process of gas injection, the injection pressure will not decrease with the increase in borehole depth. The gas pressure in the borehole stays constant. (5) Gas in the coal seam has a constant composition.

3.2.2. Model and Boundary Conditions. Although boring holes and injecting N_2 into coal seam to displace methane are three-dimensional processes in spacing, considering the feasibility and effectiveness of numerical calculations, we simplify it to a two-dimensional problem, selecting the vertical direction of the borehole as the research direction. The numerical model is shown in Figure 1.

The initial and boundary conditions of the model are as follows:

(1) The original CH_4 pressure of coalbed is p_0, and the N_2 pressure is 0

$$p_1(x, y, t)|_{t=0} = p_0,$$
$$p_2(x, y, t)|_{t=0} = 0. \quad (8)$$

(2) The model boundary flow is 0, the atmospheric pressure of the mine is 0.1 MPa, and N_2 injection pressure is set to 0.5 MPa

The engineering conditions need to be simulated as follows. The excavation roadway is 4 m high. The borehole radius is set to 90 mm in the model. There is a no flow rate boundary around the model. The injection borehole pressures are 0.5 MPa, 0.8 MPa, 1.2 MPa, and 2.0 MPa. Parameters of physical properties in numerical simulation are obtained from the laboratory data of coal samples in Shigang Coal Mine, as shown in Table 1.

3.3. Numerical Simulation and Analysis on Radius Influence of Injecting N_2. Usually, before injecting N_2 into coal seam, N_2 content in coal seam was very low. Therefore, to simplify numerical simulation, N_2 content in coal seam was ignored. Figure 2 shows the results of 0.5 MPa gas injection pressure, at different times around the bore-borehole-pressure N_2 cloud. It can be seen from Figure 2 that, with the gas injection time extended, N_2 pressure range gradually increased; therefore, the range in which the N_2 pressure rises from 0 to 0.05 MPa is defined as the influence radius of the gas injection.

At an injection pressure of 0.5 MPa, the trend of the N_2 pressure in the direction along the *O-A* line in the model is shown in Figure 3. Before injection, the N_2 pressure around the borehole is 0 Pa. As the injection time increases, the influence area of N_2 near the coal wall increases too. After 1 h gas injection, the influence radius of N_2 reaches 0.75 m. After 4 h, the influence radius of N_2 reaches 1.40 m. After 10 h, the influence radius of N_2 reaches 2.10 m. The trend of the N_2 pressure in the direction perpendicular to the *O-A* line in the model is shown in Figure 4. Before injection, the N_2 pressure around the borehole is 0 Pa. As the injection time increases, the influence area of N_2 near the coal wall increases too. After 1 h gas injection, the influence radius of N_2 reaches

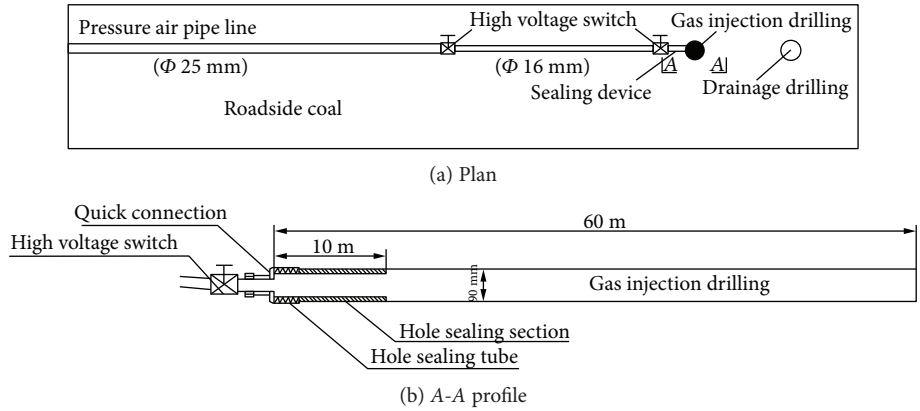

Figure 6: Diagram of gas injection.

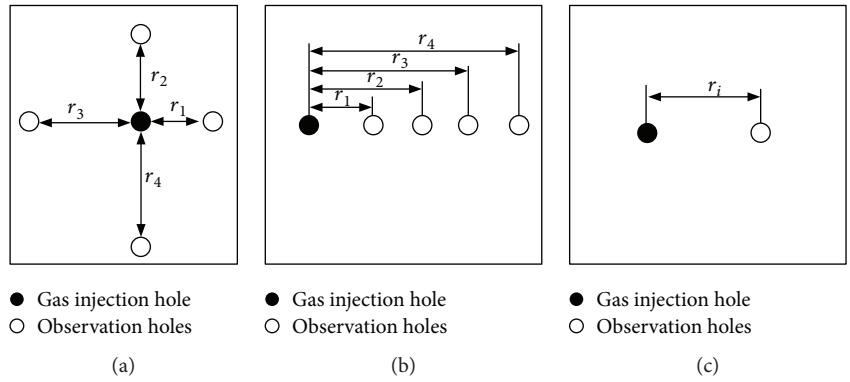

Figure 7: Borehole arrangement in the effective gas injection radius test.

Table 3: Borehole parameters in the injecting N_2 influence radius test.

Borehole type	Specifications and sealing requirements of borehole			
	Depth (m)	Diameter (mm)	Sealing depth (m)	Sealing method
N_2 injection borehole	60	94	10	Rigid PVC pipe + polyurethane entire section borehole sealing
Observation borehole	60	94	10	Rigid PVC pipe + steel pipe + polyurethane borehole sealing
Borehole spacing (m)				r_i = 0.8, 1, 1.5, 2, 3

0.63 m. After 4 h, the influence radius of N_2 reaches 1.23 m. After 10 h, the influence radius of N_2 reaches 1.85 m.

From the numerical simulation results, the difference of the influence radius of the gas injection in horizontal direction (bedding direction) and in vertical direction (vertical bedding direction) existed. The radius of the gas injection in the vertical bedding direction is smaller than that in the bedding direction, and the difference is related to the existence of the power of the gas injection time, $\Delta R = 0.1195\ t^{0.272}$. The differences are shown in Table 2 and Figure 5.

4. Field Test of Influence Radius by Injecting N_2 to Displace Coalbed Methane

4.1. Test System. In this paper, Shigang Coal Mine is selected to carry out the test. The Shigang Coal Mine is located in the northeast of the Qinshui Basin in China. The basic situation is shown in Section 3.1.

An injecting N_2 system consists of the connecting pipe, quick joint, borehole sealing device, high pressure switch, pressure gauge, etc., as shown in Figure 6. The field test gas source is nitrogen, which is provided by the mine pressure duct road. The connecting lines are composed of 25 mm high-pressure pipes. The borehole sealing device uses a hard PVC tube and polyurethane sealing, and borehole sealing pipe is connected by quick connectors.

4.2. Test of Borehole Arrangement. The borehole arrangement is shown in Figure 7. Because of the small roadway cross section in the Shigang Coal Mine, it is hard to construct two observation boreholes that are perpendicular to the coal seam. Thus, it is impossible to achieve "around holes" (Figure 7(a)). If "parallel holes" are used (Figure 7(b)), the

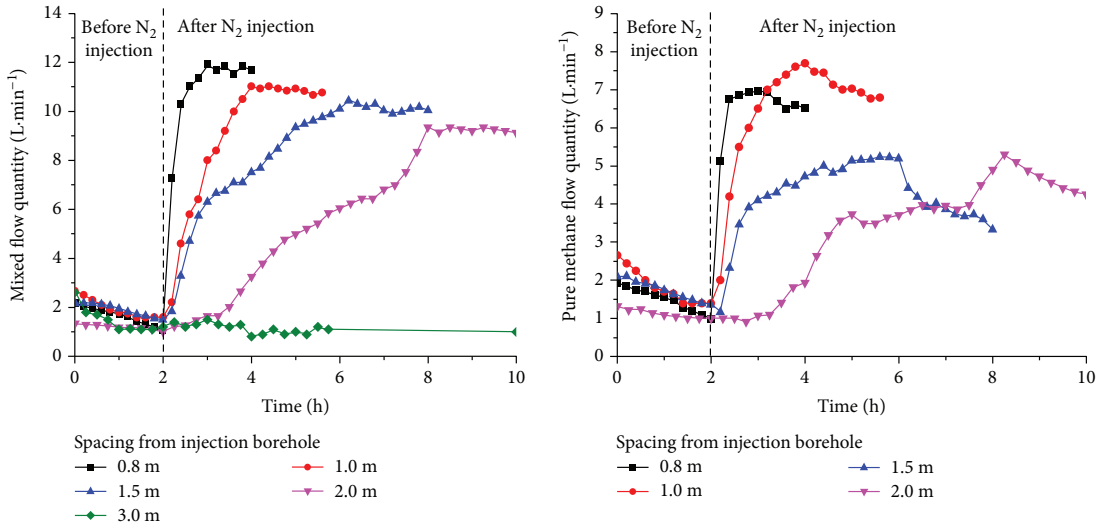

(a) Mixture flow (b) Pure flow

Figure 8: Flow change of releasing borehole at different spacing.

observation boreholes near the injection boreholes have a "closure" effect on the observation boreholes far from the injection boreholes, which may cause low or zero flow rates in the observation boreholes far from the injection boreholes. Thus, to avoid "closure" and to consider the convenience and accuracy of borehole construction, a single measuring borehole arrangement is adopted (Figure 7(c)). By enlarging the spacing between injection boreholes and observation boreholes, the influence radii at different times are measured. The design of the borehole parameters is shown in Table 3.

4.3. Test Result and Analysis. After discharging the borehole continuously for approximately 12 h, the field gas injection started. The flow rate before gas injection was balanced. In the process of gas injection, the gas injected in a coal seam accumulated in the coal, and then it formed a large pressure difference between injection borehole and discharge ?borehole, so the coalbed methane moved from the high-pressure side (injection borehole) to the low-pressure side (discharge borehole). At an early stage of gas injection, the flow rate of discharge borehole increased obviously. As the injection time increased, the flow rate of discharge borehole tended to rise steadily in spite of some local instability until the maximum mix flow rate of discharge borehole appeared. Then, the data were measured continuously with the variation of not more than 5%. The data variation condition of each group is shown in Figure 8.

It can be seen from Figure 8, when the spacing between the injection borehole and the discharge borehole is 0.8 m, the mix flow rate reached the peak of 12.08 L/min after 1 h. When the spacing between the injection borehole and the discharge borehole is 1 m, the mix flow rate reached the peak of 11.11 L/min after 2 h. When the spacing between the injection borehole and the discharge borehole is 1.5 m, the mix flow rate reached the peak of 10.52 L/min after 4 h. When the spacing between the injection borehole and the discharge borehole is 2 m, the mix flow rate reached the peak of 9.15 L/min after 7 h. When the spacing between the injection borehole and the discharge borehole is 3 m, the mix flow rate does not appear within 10 h. This observation means that when the injection pressure is 0.5 MPa, after 10 h of injection, the influence radius is less than 3 m. The field test data are shown in Table 4.

Table 4: Test results for the influence radius.

N_2 injection time (h)	N_2 injection influence radius (m)	Increase radius before and after N_2 injection flow rate
1	0.8	10.9
2	1.0	6.7
4	1.5	6.6
7	2.0	7.2

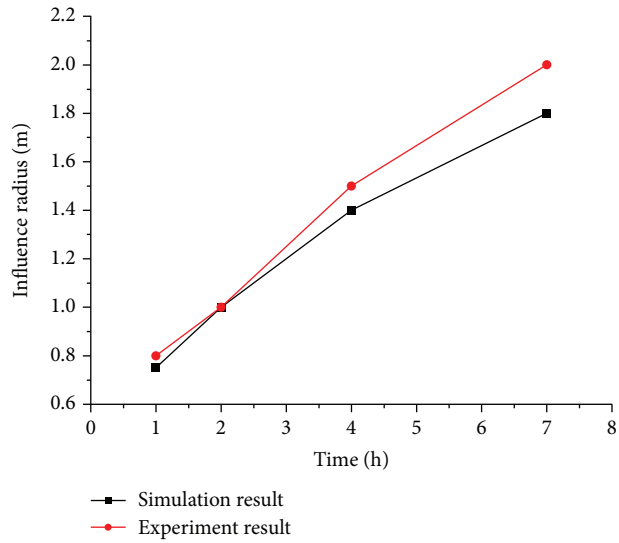

Figure 9: Influence radius under 0.5 MPa N_2 injection pressure.

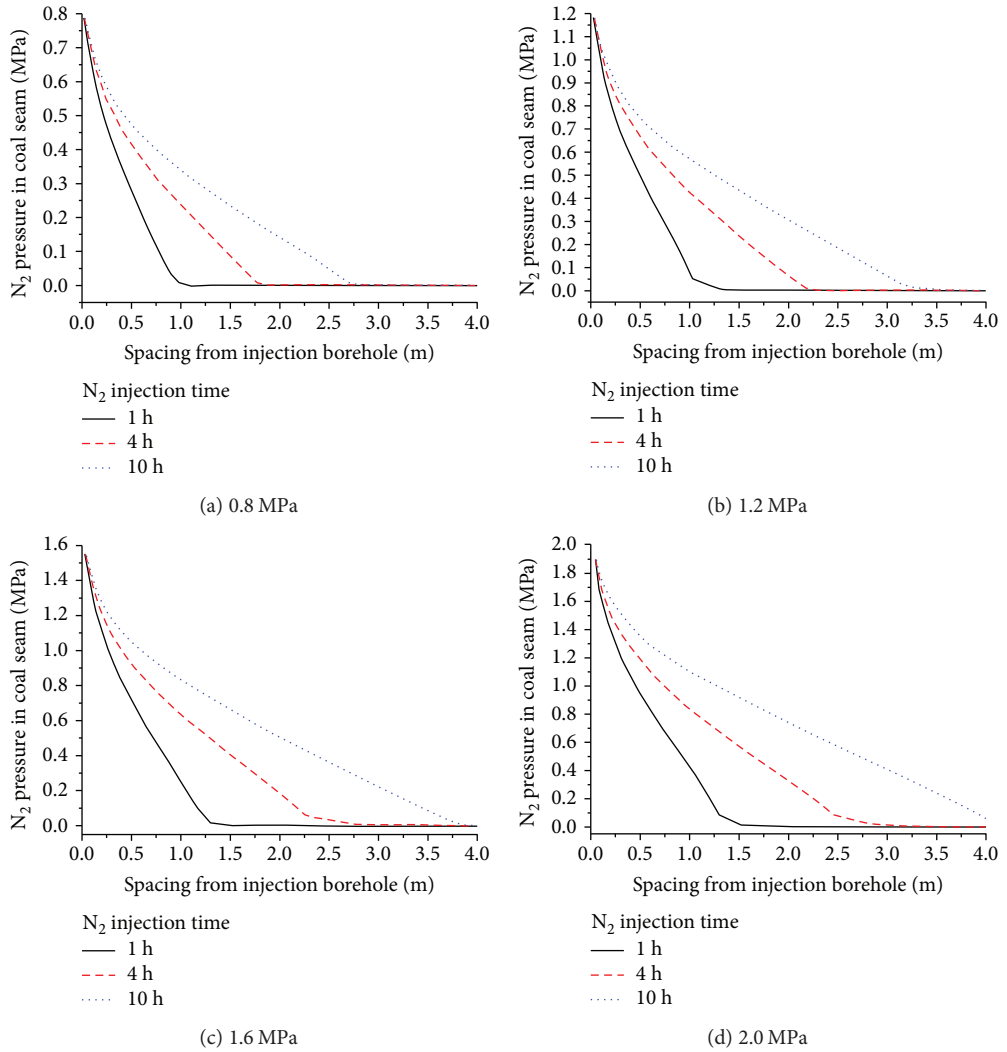

Figure 10: N_2 pressure along *O-A* direction under different gas injection pressures.

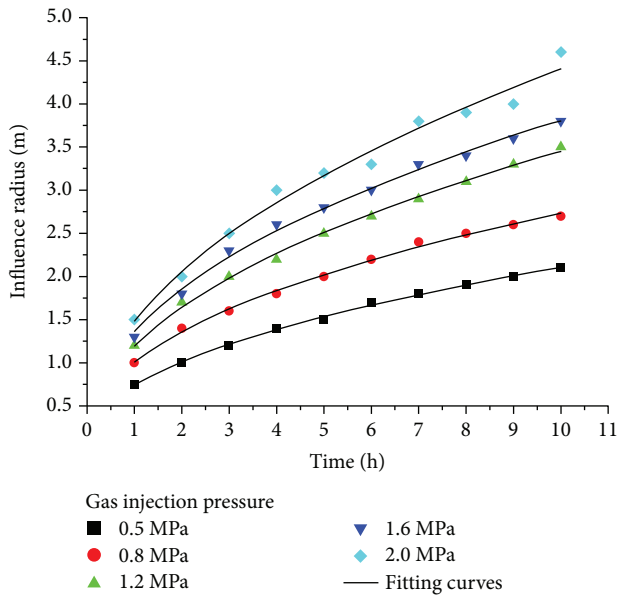

Figure 11: Influence radius under different gas injection pressures.

Table 5: The fitting formula and fitting coefficient.

Gas injection pressure (MPa)	$r = At^B$	A	B	R^2
0.5	$r = 0.7245t^{0.438}$	0.7495	0.446	0.99803
0.8	$r = 0.9947t^{0.4491}$	0.9947	0.4491	0.99641
1.2	$r = 1.2072t^{0.4544}$	1.2072	0.4544	0.99729
1.6	$r = 1.3294t^{0.4605}$	1.3294	0.4605	0.99522
2.0	$r = 1.4878t^{0.4704}$	1.4878	0.4704	0.98169

Table 4 shows that the influence radius increases as the injection time increases. However, as the injection time increases, the increase in the gas injection influence radius per unit time decreases. When the influence radius increases from 1.5 m to 2.0 m, the injection time increases by 3 h, while at the same time, the influence radius increases by only 0.5 m.

The results of the numerical simulation and the field test are shown in Figure 9. The influence radius measured by numerical simulation is close to the influence radius

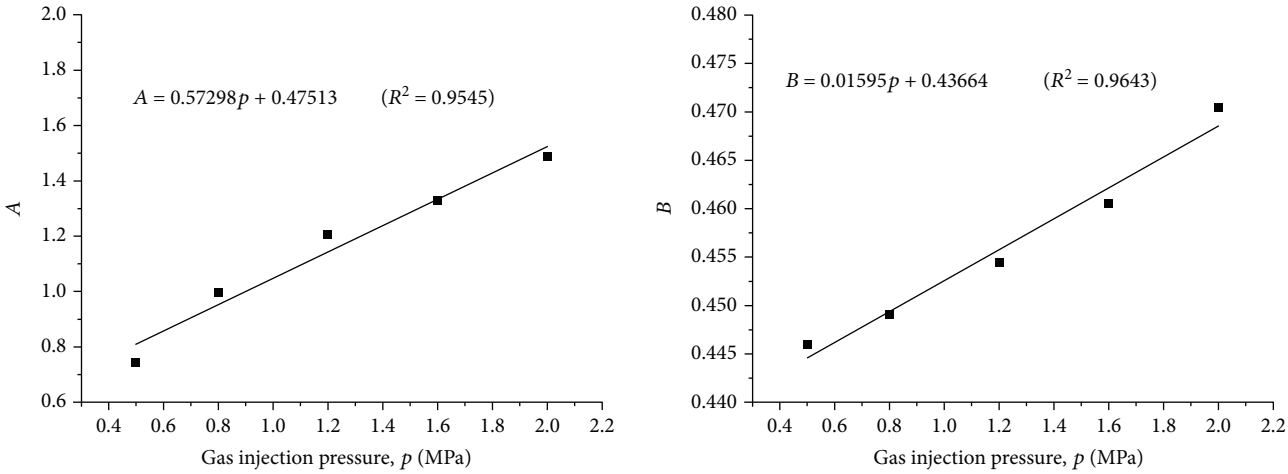

Figure 12: Coefficients of A and B under different gas injection pressures.

measured from the field test. Field test results are slightly higher than the results of numerical simulation because the model in numerical simulation is simplified, and the fissure in the coal, which may have an influence on the permeability, is ignored. Because the results of numerical simulation and the field test have consistency, the numerical model and the simulation may be considered reliable.

5. Reasonable Arrangement of Borehole

5.1. Influence Radius of Borehole under Different Injection Pressures. Adopting the numerical model above, by changing the injection pressure, the impact of the injection pressure on the influence radius of the gas injection is studied, as we can see in Figure 10. At other injection pressures, the N_2 pressure around the boreholes has the same properties as when the injection pressure is 0.5 MPa. The influence radius increases with increasing time. When the injection pressure is 0.8 MPa, the N_2 influence radius reaches 1 m after 1 h of injection. The N_2 influence radius reaches 1.8 m after 4 h of injection. The N_2 influence radius reaches 2.7 m after 10 h of injection. When the injection pressure is 1.2 MPa, the N_2 influence radius reaches 1.2 m after 1 h of injection. The N_2 influence radius reaches 2.2 m after 4 h of injection. The N_2 influence radius reaches 3.5 m after 10 h of injection. When the injection pressure is 1.6 MPa, the N_2 influence radius reaches 1.3 m after 1 h of injection. The influence radius of N_2 reaches 2.6 m after 4 h of injection. The influence radius of N_2 reaches 3.8 m after 10 h of injection. When the injection pressure is 2.0 MPa, the influence radius of N_2 reaches 1.5 m after 1 h of injection. The influence radius of N_2 reaches 3.0 m after 4 h of injection. The influence radius of N_2 reaches 4.6 m after 10 h of injection.

Meanwhile, from Figure 10, it can be seen that under the condition of equal injection time, the higher the injection pressure, the greater the influence radius will be. At injection pressures of 0.8 MPa, 1.2 MPa, 1.76 MPa, and 2.0 MPa, the influence radii reach 1 m, 1.2 m, 1.3 m, and 1.5 m, respectively, after 1 h. The influence radii reach 1.8 m, 2.2 m, 2.6 m, and 3.0 m, respectively, after 4 h. The influence radius under different injection pressures and injection times is shown in Figure 11. Their relation can be fitted by power exponents. The fitting parameters are shown in Table 5. The degree of fitting reaches to over 0.98.

Table 6: Comparison of the calculation results and the test results.

Gas injection time (h)	Radius of field test (m)	Radius of numerical simulation (m)	Error	Formula (11) radius (m)	Relative error
1	0.8	0.75	6.25%	0.76	4.80%
2	1.0	1.0	0	1.04	3.65%
4	1.5	1.4	6.67%	1.41	5.96%
7	2.0	1.8	10%	1.81	9.54%

$$r = At^B. \tag{9}$$

Injection pressure is an important factor in the influence radius. A and B are coefficients of the influence radius fitting formula for gas injection, and the relation between the two coefficients and the injection pressure p is shown in Figure 12. Coefficients A and B are both linear with respect to the injection pressure p. Plugging the relation between A and B into formula (9) yields the formula for the variation of the influence radius with time under different injection pressures.

$$r = (0.57298p + 0.47513)t^{0.01593p+0.43664}. \tag{10}$$

In order to verify the calculation formula (10), the reliability, through the formula at 0.5 MPa gas injection radius of influence of different conditions of gas injection time and with the results of the field test and numerical simulation results, was analyzed, as shown in Table 6. As can be seen from Table 6, both the numerical simulation results, or using the fitting formula (10), calculation results are consistent with the results of the field test; the error does not exceed 10%.

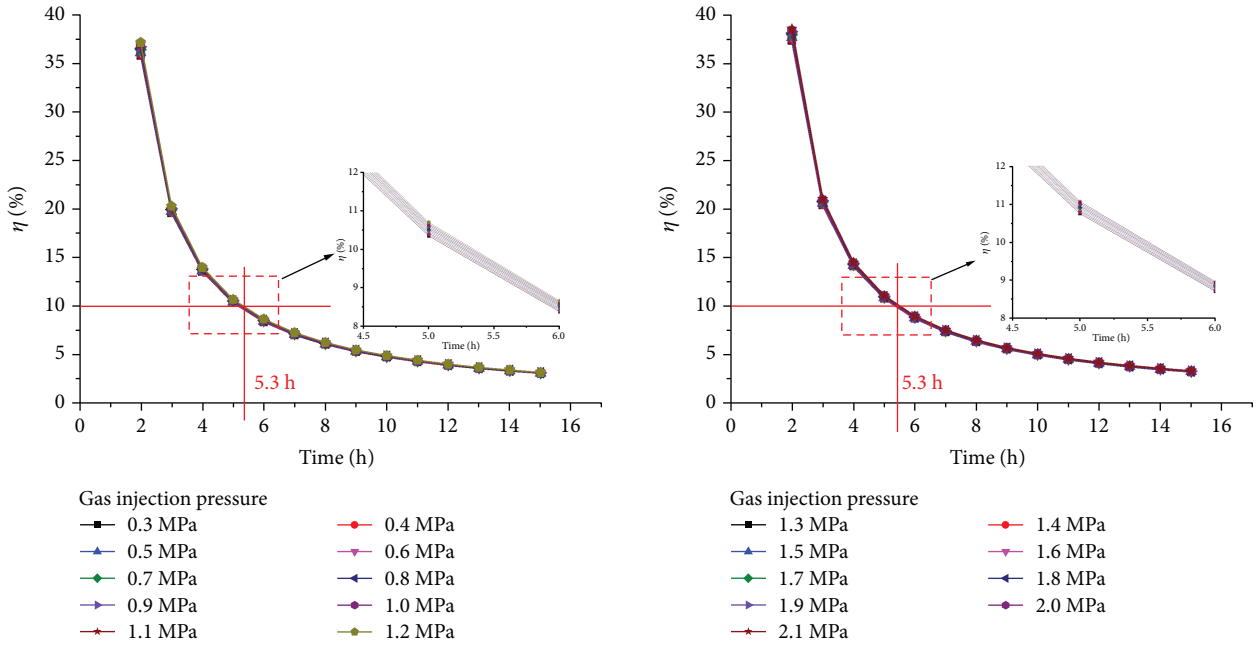

Figure 13: Increment rate of Influence radius under different gas injection pressures.

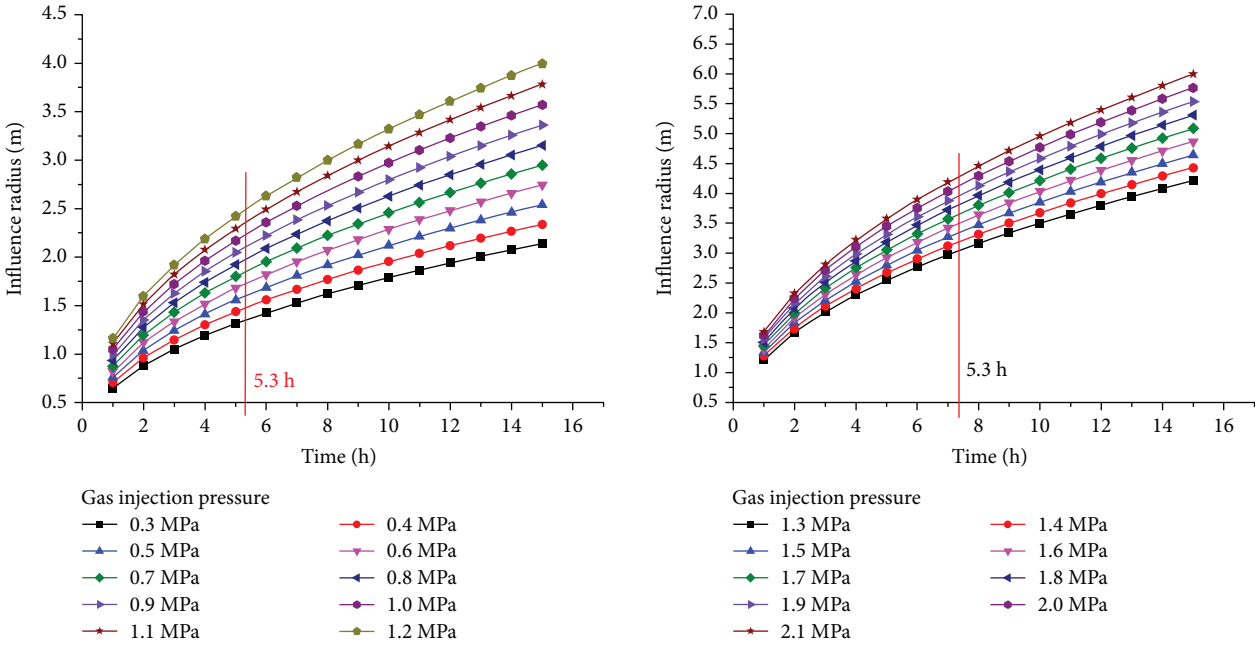

Figure 14: Influence radius under different gas injection pressures.

5.2. Reasonable Arrangement. To determine reasonable parameters for injection borehole, the increasing rate of influence radius under different injection pressures is calculated using the quantitative relation formula (11) between influence radius and injection time and injection pressure, as shown in Figure 13.

$$\eta = \frac{r_{j+1} - r_j}{t_{j+1} - t_j} \times 100\%. \tag{11}$$

In the formula, r_{j+1} and r_j are the influence radii at times t_{j+1} and t_j. η is the increasing rate of influence radius from time t_j to time t_{j+1}.

From Figures 13 and 14, it can be seen that the influence radius of the gas injection increases with the injection time, but the increment decreases with time. Thus, the increment of the influence radius per unit time will decrease to the limit as time increases. This observation means that if the injection time is long enough, the

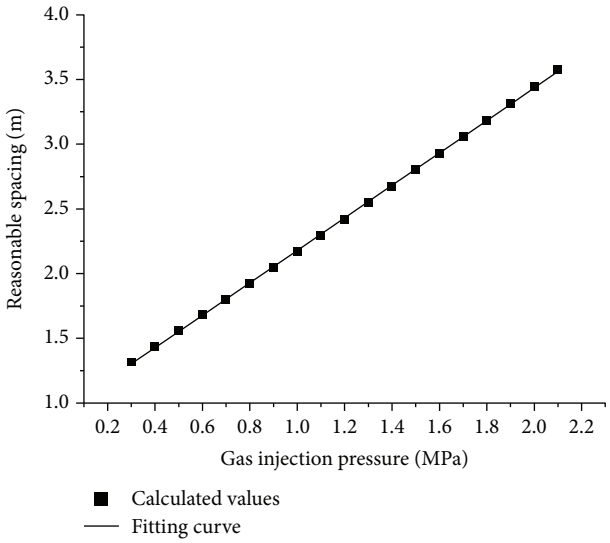

Figure 15: Reasonable spacing between N_2 injection borehole and N_2 drainage borehole under different N_2 injection pressures.

influence radius will not increase even though the injection time continues to increase. When the increment of the influence radius is less than 5% per unit time, further increases in time are unnecessary. To improve the field injection efficiency and ensure that the gas will discharge quickly after drill hole, the borehole arrangement used in the field adopts 10% as the rate increases. As shown in Figure 13, the injection time is approximately 5.3 h. From Figure 14, a reasonable spacing between injection borehole and discharge borehole is obtained. For the Shigang no. 15 coal seam, when the injection pressure is 0.5 MPa, the calculated reasonable spacing between injection borehole and discharge borehole is 1.56 m, and we used 1.6 m in the field test. For other injection pressures, the reasonable spacing between injection borehole and discharge borehole is shown in Figure 15. Their reasonable spacing L is linearly correlated with pressure p, and the relation can be represented as follows:

$$L = 0.924 + 1.255p, \quad R^2 = 0.9998. \tag{12}$$

6. Conclusions

Based on numerical simulation and field test analysis of the time characteristics of the injecting N_2 influence radius, we conclude the following:

(3) The influence radius and injection time can both be expressed as exponents, and their fitting degrees are linear with injection pressure. Based on this and the results obtained from the relation between the influence radius and the injection time, the pressure tends to agree with the results obtained from the field test. The difference is no more than 10%

(4) Reasonable spacing between injection boreholes and discharge boreholes can be determined from the increasing rate of the influence radius. When the increasing rate of the influence radius is less than 10%, the influence radius is the reasonable spacing of the boreholes. Using this method, the reasonable spacing between the injection borehole and the discharge borehole at Shigang Coal Mine was determined to be 1.56 m, and 1.5 m was used for the field test

(5) At different injection pressures, the reasonable spacing between injection boreholes and discharge boreholes tend to be linearly related to the injection pressure

Data Availability

The data used to support the findings of this study are available from the corresponding author upon request.

Conflicts of Interest

The authors declare that they have no conflicts of interest.

Acknowledgments

This work was carried out with funding from the National Natural Science Foundation of China (Grant nos. 51174081 and 51404091).

Supplementary Materials

Original record of the field experiment that will support the conclusion of the article. *(Supplementary Materials)*

References

[1] R. M. Cuéllar-Franca and A. Azapagic, "Carbon capture, storage and utilisation technologies: a critical analysis and comparison of their life cycle environmental impacts," *Journal of CO2 Utilization*, vol. 9, pp. 82–102, 2015.

[2] L. Wang and B. Jiang, "Experimental study of the effect of static water on imbibition gas recovery in coalbed methane reservoirs," *Journal of Natural Gas Science and Engineering*, vol. 35, pp. 1284–1292, 2016.

[3] F. He, W. P. Linak, S. Deng, and F. Li, "Particulate formation from a copper oxide-based oxygen carrier in chemical looping combustion for CO_2 capture," *Environmental Science & Technology*, vol. 51, no. 4, pp. 2482–2490, 2017.

[4] N. Mallick and V. Prabu, "Energy analysis on Coalbed Methane (CBM) coupled power systems," *Journal of CO2 Utilization*, vol. 19, pp. 16–27, 2017.

[5] Y. Zhao, Y. Feng, and X. Zhang, "Selective adsorption and selective transport diffusion of CO_2–CH_4 binary mixture in coal ultramicropores," *Environmental Science & Technology*, vol. 50, no. 17, pp. 9380–9389, 2016.

[6] X. Tang and N. Ripepi, "High pressure supercritical carbon dioxide adsorption in coal: adsorption model and thermodynamic characteristics," *Journal of CO2 Utilization*, vol. 18, pp. 189–197, 2017.

[7] A. Shahtalebi, P. Shukla, A. H. Farmahini, and S. K. Bhatia, "Barriers to diffusion of CO_2 in microporous carbon derived from silicon carbide," *Carbon*, vol. 88, pp. 1–15, 2015.

[8] A. S. Ranathunga, M. S. A. Perera, P. G. Ranjith, X. G. Zhang, and B. Wu, "Super-critical carbon dioxide flow behaviour in low rank coal: a meso-scale experimental study," *Journal of CO2 Utilization*, vol. 20, pp. 1–13, 2017.

[9] R. R. Scott, "The Coal-Seq project: key results from field, laboratory, and modeling studies," in *Proceedings of the 7th International Conference on Greenhouse Gas Control Technologies*, pp. 1399–1403, Vancouver, Canada, 2005.

[10] R. Puri and D. Yee, "Enhanced coalbed methane recovery," in *Society of Petroleum Engineers 65th Annual Technical Conference and Exhibition*, pp. 23–26, New Orleans, LA, USA, 1990.

[11] M. Godec, G. Koperna, and J. Gale, "CO_2-ECBM: a review of its status and global potential," *Energy Procedia*, vol. 63, pp. 5858–5869, 2014.

[12] C. R. Clarkson and R. M. Bustin, "Binary gas adsorption/desorption isotherms: effect of moisture and coal composition upon carbon dioxide selectivity over methane," *International Journal of Coal Geology*, vol. 42, no. 4, pp. 241–271, 2000.

[13] M. Weber, T. H. Wilson, B. Akwari, A. W. Wells, and G. Koperna, "Impact of geological complexity of the Fruitland Formation on combined CO_2 enhanced recovery/sequestration at San Juan Basin pilot site," *International Journal of Coal Geology*, vol. 104, no. 30, pp. 46–58, 2012.

[14] Y. Y. Liu and J. Wilcox, "Effects of surface heterogeneity on the adsorption of CO_2 in microporous carbons," *Environmental Science & Technology*, vol. 46, no. 3, pp. 1940–1947, 2012.

[15] F. Van Bergen, H. J. Pagnier, L. G. Van der Meer, F. J. Van den Belt, P. L. Winthaegen, and R. S. Westerhoff, "Development of a field experiment of CO_2 storage in coalbeds in the Upper Silesian Basin of Poland," in *Proceedings of 6th Conference on Greenhouse Gas Control Technologies (GHGT6)*, pp. 569–574, Kyoto, Japan, 2002.

[16] China United Coalbed Methane Corporation, Ltd Written, *China's CBM Exploration and Exploitation Technical Researches*, Petroleum Industry Press, Beijing, China, 2007.

[17] Z. M. Fang, X. C. Li, and H. Li, "Feasibility study of gas mixture enhanced coalbed methane recovery technology," *Rock and Soil Mechanics*, vol. 31, no. 10, pp. 3223–3229, 2010.

[18] H. M. Yang, T. G. Zhang, Z. F. Wang, and C. C. Zhao, "Experimental study on technology of accelerating methane release by nitrogen injection in coalbed," *Journal of China Coal Society*, vol. 30, no. 5, pp. 792–796, 2010.

[19] W. D. Gunter, T. Gentzis, B. A. Rottenfusser, and R. J. H. Richardson, "Deep coalbed methane in Alberta, Canada: a fuel resource with the potential of zero greenhouse gas emissions," *Energy Conversion and Management*, vol. 38, pp. S217–S222, 1997.

[20] S. SH, L. Schoeling, and L. Pekot, "CO_2 injection for enhanced coalbed methane recovery: project screening and design," in *Proceedings of the 1993 International Coalbed Methane Symposium*, Tuscaloosa, AL, USA, 1999.

[21] X. Cui, R. M. Bustin, and G. Dipple, "Selective transport of CO_2, CH_4, and N_2 in coals: insights from modeling of experimental gas adsorption data," *Fuel*, vol. 83, no. 3, pp. 293–303, 2004.

[22] B. Dutka, M. Kudasik, and J. Topolnicki, "Pore pressure changes accompanying exchange sorption of CO_2/CH_4 in a coal briquette," *Fuel Processing Technology*, vol. 100, pp. 30–34, 2012.

[23] B. Dutka, M. Kudasik, Z. Pokryszka, N. Skoczylas, J. Topolnicki, and M. Wierzbicki, "Balance of CO_2/CH_4 exchange sorption in a coal briquette," *Fuel Processing Technology*, vol. 106, pp. 95–101, 2013.

[24] M. Sayyafzadeh, A. Keshavarz, A. R. M. Alias, K. A. Dong, and M. Manser, "Investigation of varying-composition gas injection for coalbed methane recovery enhancement: a simulation-based study," *Journal of Natural Gas Science and Engineering*, vol. 27, no. 2, pp. 1205–1212, 2015.

[25] H. M. Yang, C. H. Wei, Z. F. Wang, and T. H. Yang, "Numerical simulation of coal-bed methane displacement by underground gas injection based on multi-physics coupling," *Journal of China Coal Society*, vol. 35, no. 8, pp. 109–114, 2010.

[26] Z. SN and B. Q. Lin, *The Theory of Gas Flow and Storage in Coal Seams*, China Coal Industry Publishing Home, Beijing, China, 1999.